

Figure 1. Zn-(DL)DTT ( $\blacklozenge$ ); Cd-(DL)DTT ( $\blacksquare$ ); Ni-(DL)DTT ( $\blacktriangle$ ); Mn-(DL)DTT ( $\times$ ).

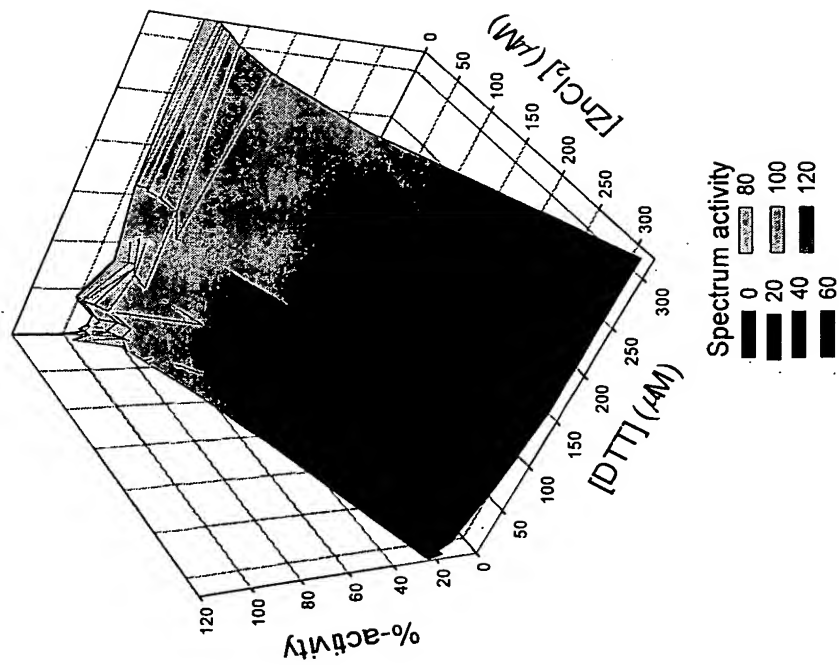


Figure 2A.

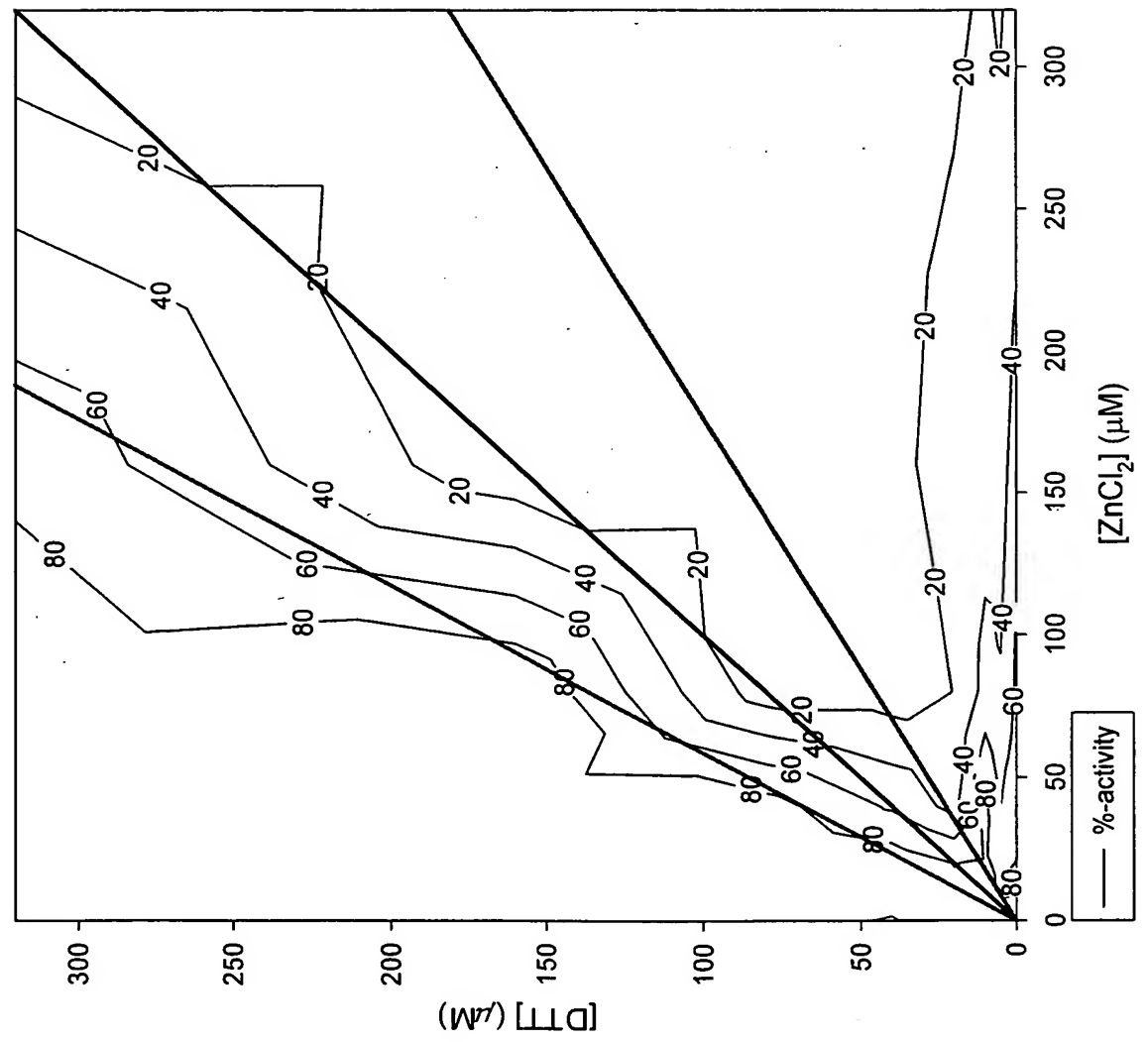
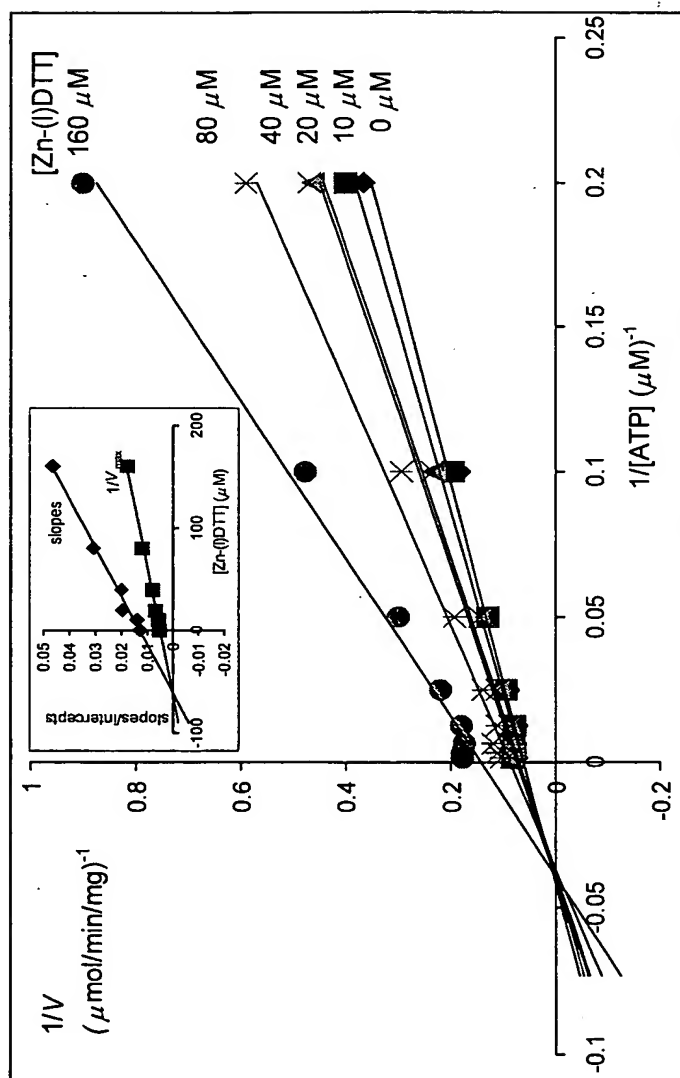
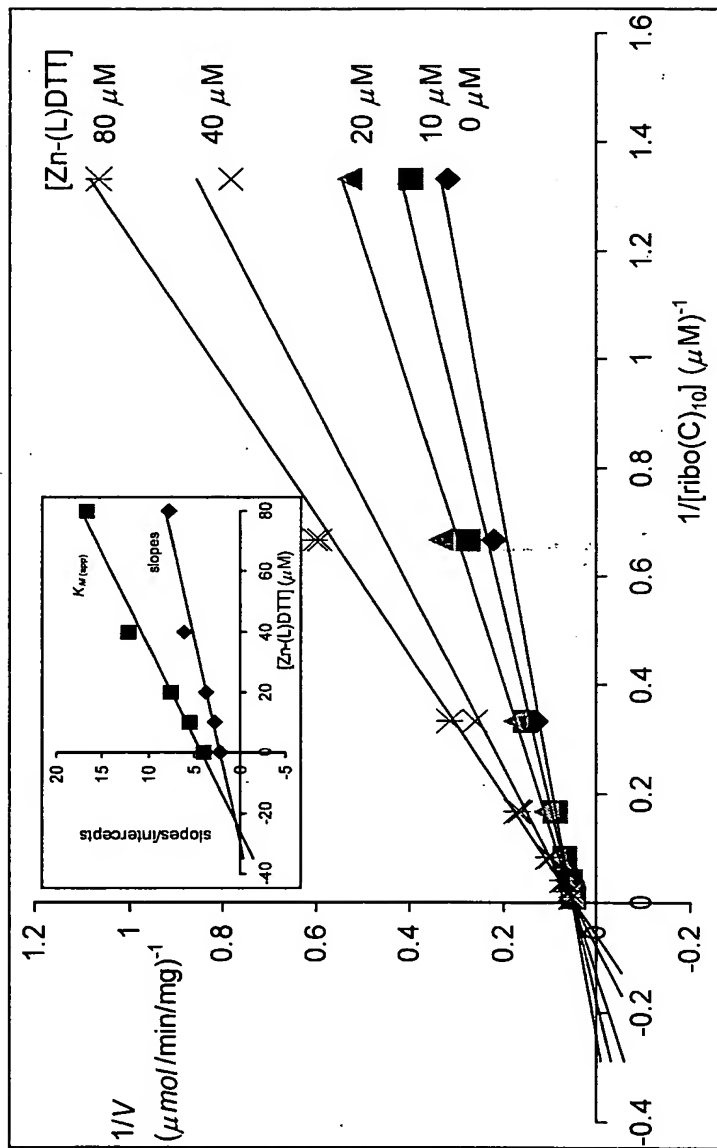


Figure 2B.



**Figure 3A.** Inset, a plot of the slopes ( $\diamond$ ) and intercepts ( $\blacksquare$ ) versus Zn-(L)DTT concentrations.



**Figure 3B.** Inset, a plot of the slopes (♦) and intercepts (■) versus  $Zn-(L)DTT$  concentrations.

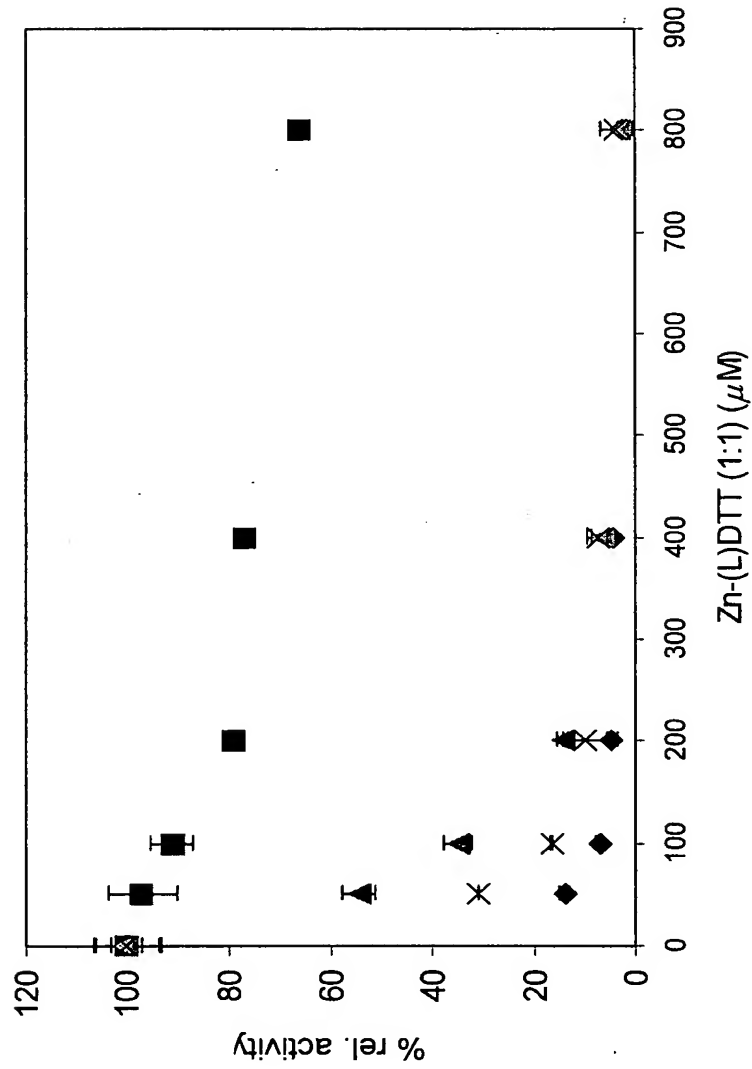


**Figure 4.** Control (♦); no preincubation (■); 10-fold concentration of rho, poly(C) and ATP (▲); standard condition + 0.1 mg/mL BSA (X).

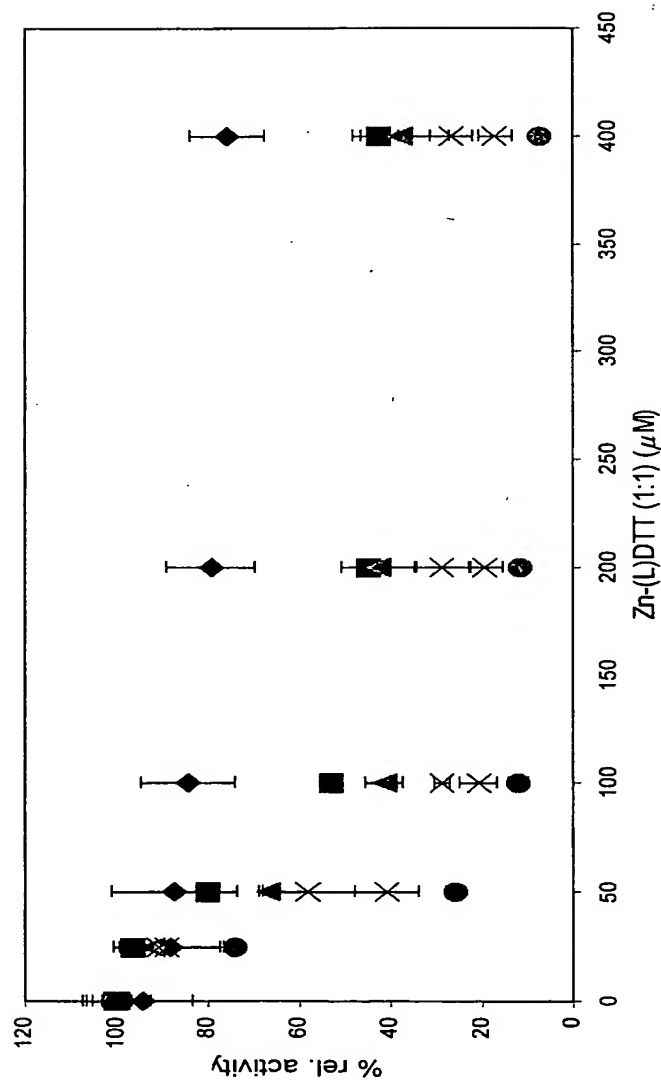
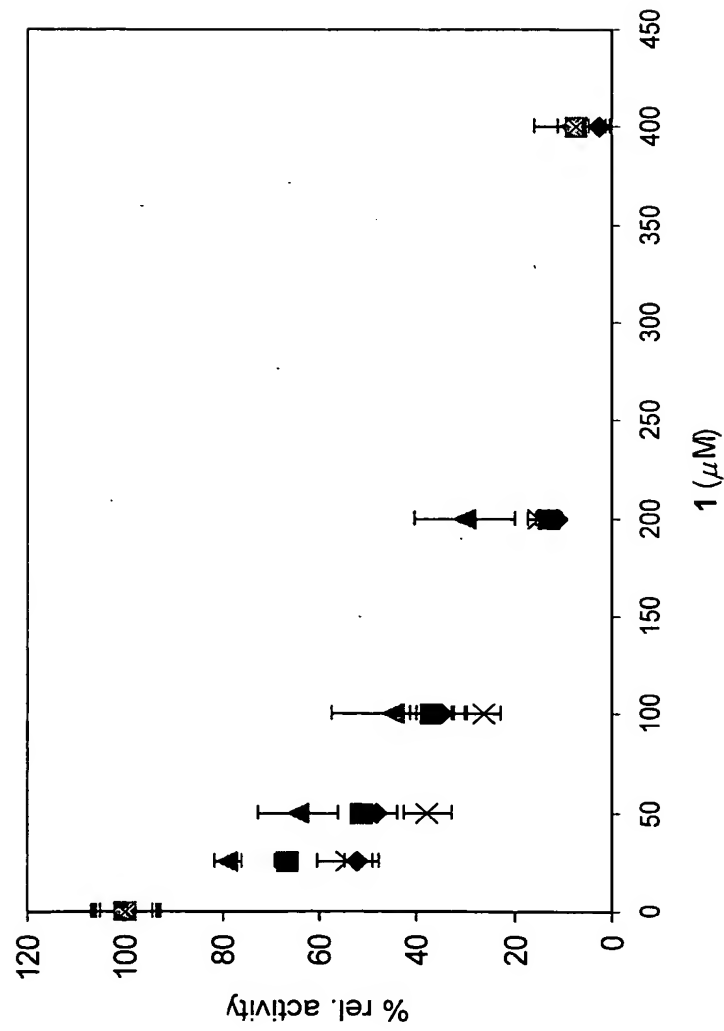


Figure 5. No preincubation ( $\blacklozenge$ ); 15 sec ( $\blacksquare$ ); 30 sec ( $\blacktriangle$ ); 1 min ( $\times$ ); 2 min ( $\times$ ); 5 min ( $\bullet$ ).



**Figure 6.** Control ( $\diamond$ ); No preincubation ( $\blacksquare$ ); 10-fold concentration of rho, poly(C) and ATP ( $\blacktriangle$ ); standard condition + 0.1 mg/mL BSA ( $\times$ ).



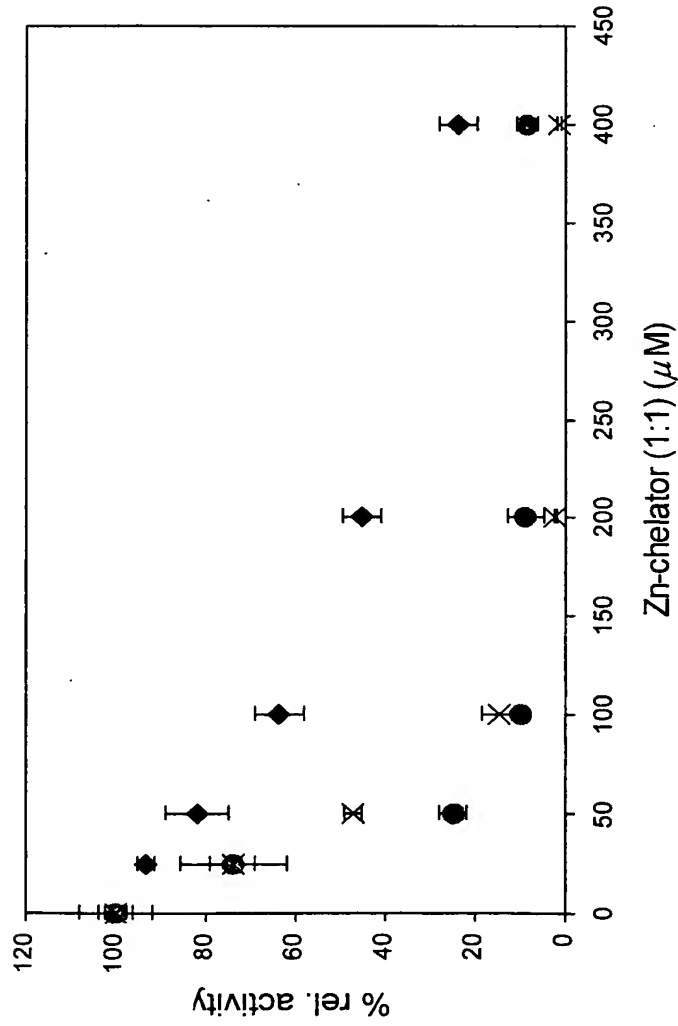
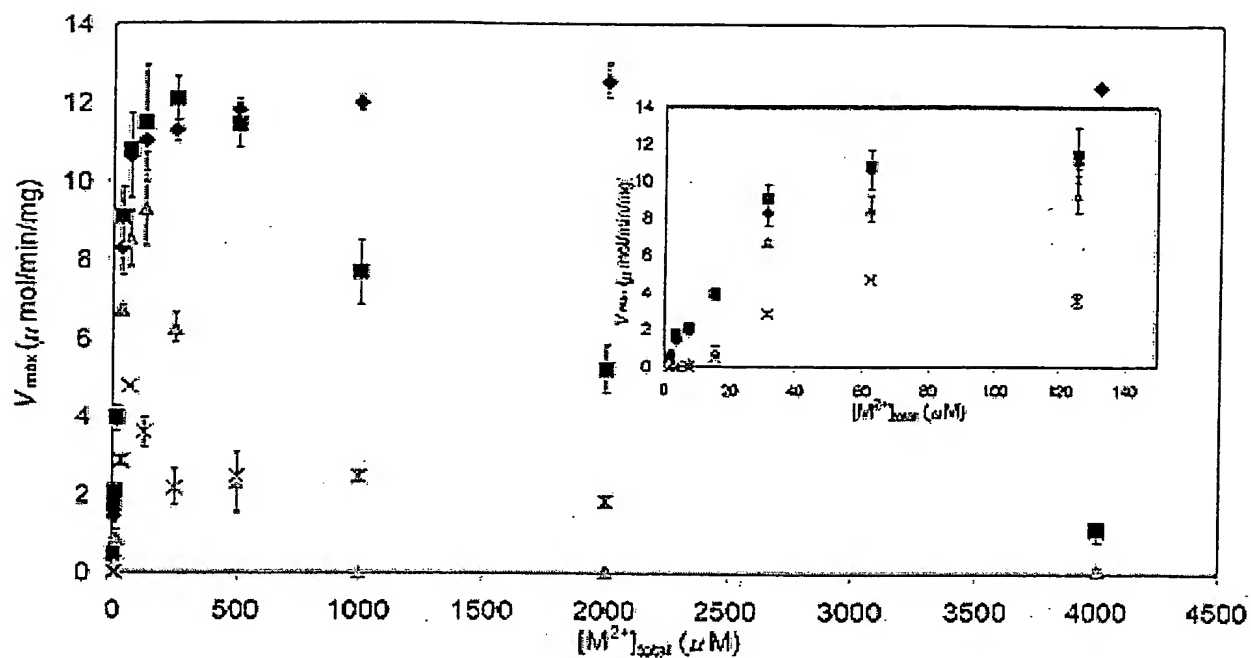


Figure 7. Zn-2-mercaptoethanol (♦); Zn-

1,2-ethanedithiol (X); Zn-(L)DTT (●).



**Figure 8.** The average velocities of two determinations are plotted with  $\text{Mg}^{2+}$  (diamonds),  $\text{Mn}^{2+}$  (squares),  $\text{Zn}^{2+}$  (gray triangles), and  $\text{Cd}^{2+}$  (x). The inset shows metal activation of rho exhibiting a peak velocity and sigmoidal behavior at rho divalent metal concentrations.